Rep. Fac. Sci., Kagoshima Univ.,
No. 56, pp. 9-18 (2023)

Petrography, textural and chemical characteristics of carbonatites from northwest Himalayas Pakistan

Mehboob ur RASHID[1)], Hafiz U. REHMAN[1)*], Hiroshi YAMAMOTO[1)], Muhammad Jawad ZEB[2)]

[1)] Graduate School of Science and Engineering, Kagoshima University, Kagoshima 890-0065

[2)] Geoscience Advance Research Labs, Geological Survey of Pakistan 44000

* hafiz@sci.kagoshima-u.ac.jp

Abstract: This study investigates the mineralogical, textural, and compositional variations within the carbonatite bodies exposed in the Peshawar Plain Alkaline Igneous Province (PPAIP), northwest Himalayas, Pakistan. A comprehensive methodology combining elemental mapping using the X-ray guided tube, petrography, and X-ray fluorescence (XRF) analysis was employed to characterise four distinct carbonatite varieties: Jambil, Sillai Pattai, Loe Shilman, and Warsak. The results reveal notable mineralogical variations among the studied carbonatite bodies, with calcite as the predominant phase. However, associated minerals vary significantly, reflecting distinct geological processes that formed the carbonatite bodies. The geochemical data obtained through XRF analysis elucidate the composition of major oxides and trace elements, providing insights into the petrogenesis of these carbonatites. Ternary diagrams, constructed from major oxides ca. CaO-MgO-FeO, confirm their classification dominantly as calcio carbonatites with some transition towards ferro carbonatites. These findings enhance our understanding of the formation and evolution of carbonatite complexes in the PPAIP and contribute valuable insights into the geological history of this region.

Keywords: Carbonatites, PPAIP, northwest Himalaya, petrography, elemental mapping, geochemical composition

1. Introduction

Carbonatites are intrusive and extrusive igneous rocks with a model composition of more than 50% carbonate and less than 10% silica [1-3]. Calcite, dolomite, and siderite/ankerite are the most frequent minerals found in carbonatites [3,4]. Calcio carbonatites, Magnesio carbonatites, Ferro carbonatites and Natro carbonatites are the four main types of carbonatites [5]. Carbonatite occurrences have been identified in a variety of tectonic settings, with a significant prevalence in extensional environments such as continental rifts and post-collisional zones [6,7]. The origin of carbonatites is still undecided but accepted as these rocks are mainly crystallized from direct partial melting of carbonate-rich mantle or silicate-carbonate immiscibility followed by fractional crystallization of carbonate-bearing, silica-undersaturated magmas [8,9]. Carbonatites, in addition to their geological intrigue, hold colossal economic significance in terms of mineralization. Some of the world's most extensive and economically vital deposits of Iron (Fe), Niobium (Nb), and Rare Earth Elements (REEs) are found within carbonatites [8,10]. Due to their unique nature, host for REEs and their enigmatic origin researchers around the globe are attracted to study carbonatites. There are 527 known carbonatite occurrences worldwide, with 46 of them being extrusive [11]. Africa has the highest number with 171 occurrences, followed by Asia with 160 localities [11]. Carbonatite occurrences span a wide range of ages, starting from the Archean to Cenozoic times. This variation in age highlights the temporal diversity of carbonatite distribution worldwide [11].

Numerous carbonatite occurrences have been reported from the Indian subcontinent. While the majority of carbonatites are exposed in India, four localities are reported from Pakistan, two in Sri Lanka, and one from Afghanistan (Fig. 1). These occurrences range in age from Precambrian to Paleogene (Table. 1). The oldest known

carbonatites in India include the Hogenakal carbonatite in Tamil Nadu which were reported to have formed within the period between 2415 to 2401 Ma (based on Rb/Sr and Sm/Nd isochron age on whole rock [12]). Those exposed in the Newania complex in Rajasthan were reported for 2273 to 1551 Ma (based on Pb/Pb on whole rock) and 959 Ma (using the K-Ar dating on amphibole [13-15]). Whereas those exposed in the Sevathur complex in Tamil Nadu have been reported to have formed around 767 Ma (based on Rb/Sr on whole-rock) [12]. The Jurassic carbonatite (ca. 149 Ma, based on phlogopite K-Ar geochronology) activity was reported from the Sung valley [16]. The Amba Dongar complex in India dates approximately 65 Ma (based on U-Pb on apatite)[17]. In Sri Lanka, the Eppawala carbonatites were initially thought to have formed around 493 Ma (based on Rb/Sr isotope age on biotite, apatite and whole rock [18], and was later revised to 808 ± 185 Ma (based on Sm–Nd on apatite) [19]. The single carbonatite locality exposed in Afghanistan, the Khanneshin carbonatite, is the youngest among the carbonatites of Indian subcontinent, with an age value of 5 to 1.4 Ma (unpublished data [20-21]).

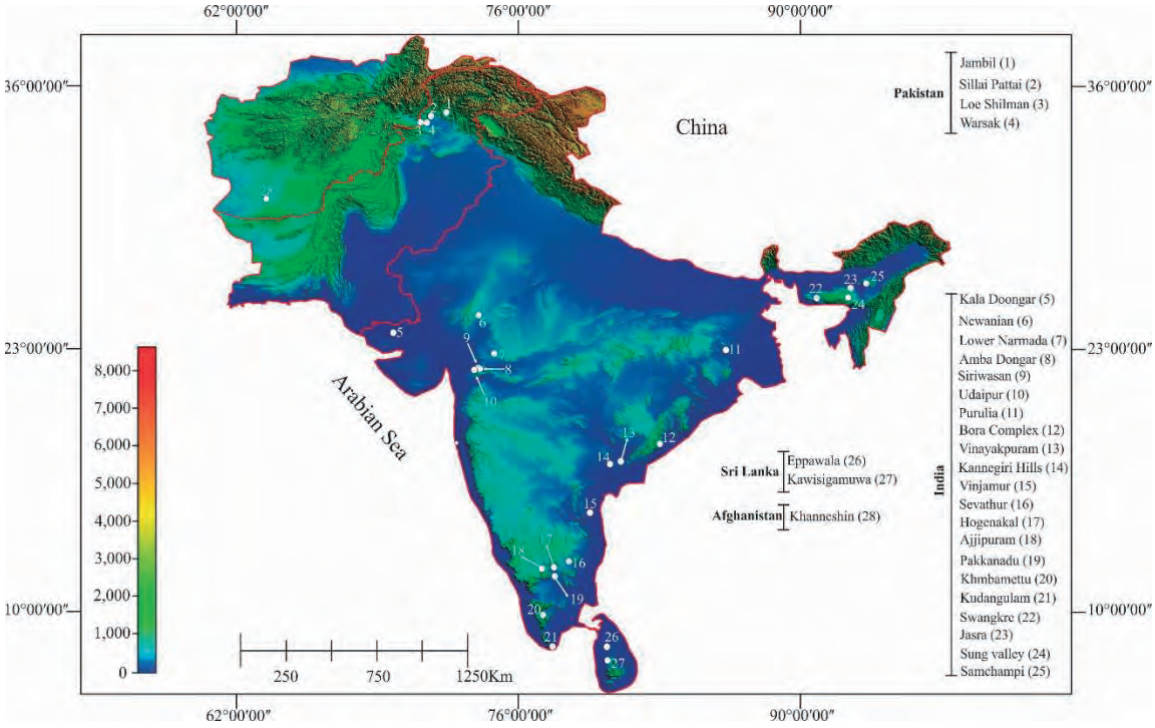

Fig. 1. Sketch map of Indian sub-continent showing location of carbonatites in India, Pakistan, Sri Lanka and Afghanistan.

In Pakistan, carbonatite occurrences are reported from Peshawar Plain Alkaline Igneous Province (PPAIP), northwest Himalayas [22] (Fig. 2). The PPAIP is having outcrop area of 1000 km^2 and stretches up to 200 km, situated at the south of a suture zone, referred as the Main Mantle Thrust (MMT) that demarcates the tectonic boundary between the Indian plate and the Kohistan island arc (Fig. 2)[22]. The Peshawar plain alkaline magmatism was reported to have produced due to the mantle plume-induced lithospheric doming associated with compression release in Permo-Carboniferous [23-24]. Carbonatites in PPAIP are exposed at four localities namely the Jambil, Sillai Pattai, Loe Shilman, and Warsak areas (Fig. 2). The emplacement of carbonatites within the PPAIP has been a subject of debate among researchers for years with various hypotheses proposed, 1) single episode of magmatism during Permo-Carboniferous [23-26], 2) two episodes, while the earlier magmatism was in Permo-Carboniferous, the second was in Paleogene [22], and 3) Plume-related magmatism associated with the Reunion hotspot in Cretaceous [27-28]. Silurian carbonatites were also reported from the PPAIP area (Table. 1). The wide age range and magmatic events associated

with the formation of carbonatites suggest complex geological history that was operative in the study area when the carbonatites were forming.

The aim of this study is to investigate mineralogical, textural, and compositional variations of the carbonatites (Jambil, Sillai Pattai, Loe Shilman, and Warsak) exposed in PPAIP in order to understand their geodynamic evolution and relation with the regional tectonic settings.

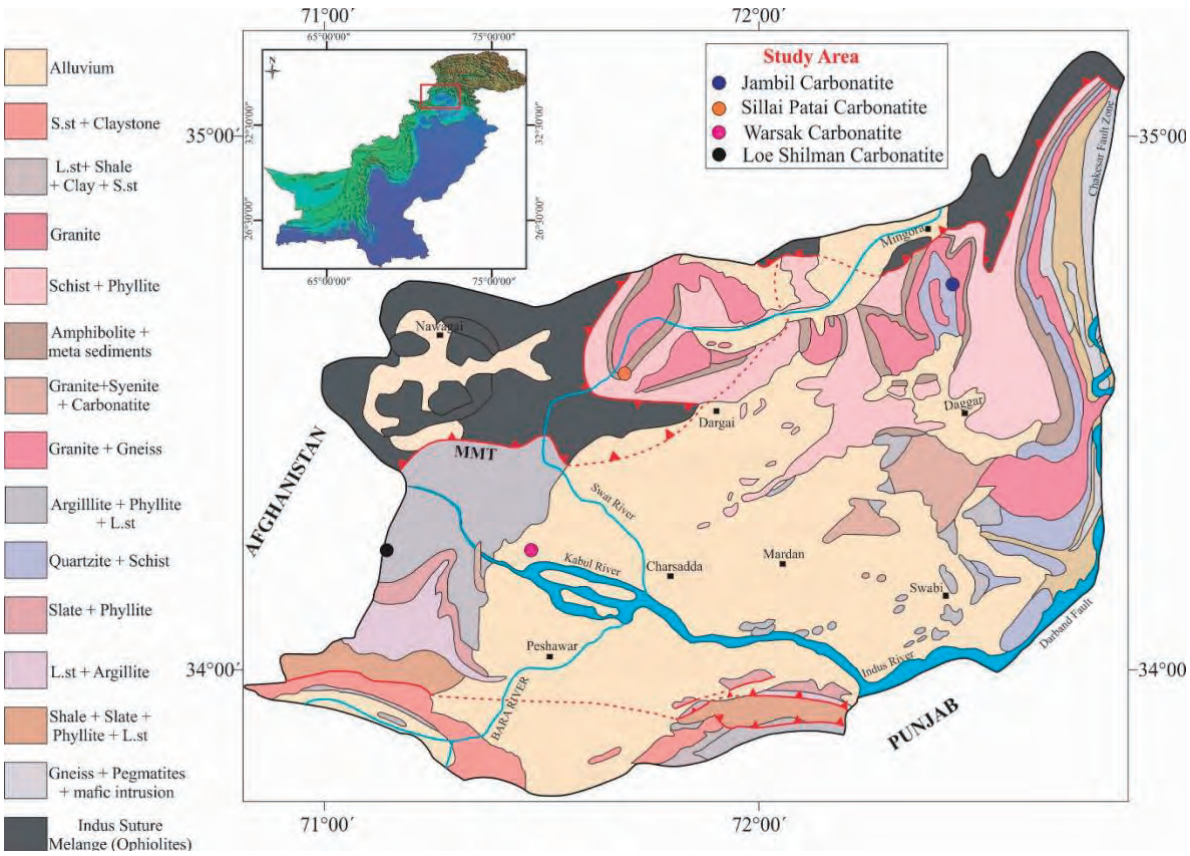

Fig. 2. Geological map of the Peshawar Plain Alkaline Igneous Province (PPAIP) showing locations of carbonatite bodies (modified from Aslam et al. [29]).

2. Materials and Methods

The methodology employed in this study is centered on the elemental mapping of major and some trace element analyses conducted on polished thin sections using the X-ray guided tube (XGT) situated at the Instrumental Analytical Center of Kagoshima University. Additionally, petrography was conducted through the examination of prepared thin sections using the optical microscopes and via the Keyence digital microscope (model VHX 8000) located at the Faculty of Science, Kagoshima University. Elemental composition analyses were performed on powdered samples using Bruker's S1 TITAN portable Handheld X-ray fluorescence (HH-XRF) spectrometer. Analysis time for each sample was 90 s in three cycles of 30 s each to measure abundance of various elements in the powdered sample. Analyses were conducted three times on each sample for confirmation and accuracy. Before and after 10 to 15 analyses, a standard reference sample (CS-M2, a stainless steel pellet with known chemical composition) was tested to maintain the measurement accuracy. The results obtained from CS-M2 were better than 98%. The obtained XRF data was subsequently processed and analyzed using the GCD-tool kit, a computer software, with a specific emphasis on the construction of a CaO-MgO-FeO ternary diagram for the purpose of classifying the studied carbonatite samples.

Table 1: Geochronological results of carbonatites exposed in the Indian subcontinent

Country	Locality	Method	Age (Ma)	References	Period
Pakistan	Jambil carbonatite	Titanite U-Pb	438	[34]	Silurian
	Jambil carbonatite	Apatite Fission track	15	[30]	Miocene
	Sillai Pattai carbonatite	Apatite Fission track	21	[31]	
	Sillai Pattai carbonatite	Apatite Fission track	29	[32]	
	Sillai Pattai carbonatite	Biotite K-Ar	31	[22]	Oligocene
	Sillai Pattai carbonatite	Zircon Fission track	32	[31]	
	Sillai Pattai carbonatite	Titanite U-Pb	83	[27]	Cretaceous
	Loe Shilman carbonatite	Apatite Fission track	30	[33]	Oligocene
	Loe Shilman carbonatite	Biotite K-Ar	31	[22]	
	Loe Shilman carbonatite	Zircon U-Pb	90	[28]	Cretaceous
India	Amba Dongar carbonatite	Apatite U-Pb	65	[17]	Paleocene
	Sung carbonatite	Phlogopite K-Ar	149	[16]	Jurassic
	Sevathur carbonatite	Whole rock Rb-Sr	767	[12]	
	Newanian carbonatite	Whole rock Pb-Pb	2273	[14]	Precambrian
	Hogenakal carbonatite	Whole rock-Rb-Sr	2415	[12]	
Sri Lanka	Eppawala carbonatite	Apatite Sm-Nd	808	[19]	Precambrian
Afghanistan	Khanneshin carbonatite	unpublished data	1.4	[20]	Pliocene

3. Results

Elemental mapping by XGT, juxtaposed with the petrological analysis, and chemical compositions depict mineralogical distribution within the studied carbonatite samples from the PPAIP.

Samples of Jambil carbonatites (JC) exhibit notably high concentrations of calcium (Ca), followed by iron (Fe) and potassium (K). In addition, there are varying but relatively low concentrations of manganese (Mn), chlorine (Cl), aluminum (Al), phosphorus (P), and titanium (Ti) (Fig. 3a). Petrographic investigation of JC revealed that the predominant minerals present are calcite and pyroxene (Fig. 4a-b). Furthermore, accessory minerals such as apatite, rutile, zircon, and diopside have been identified. The results of XGT analysis align harmoniously with the observations made through petrography. Specifically, the abundance of Ca corresponds to the presence of calcite ($CaCO_3$), Fe is indicative of aegirine-augite [($NaFeSi_2O_6$, (Ca, Na) (Mg, Fe, Al, Ti) (Si, Al)$_2O_6$)], while the Ti along with Ca indicate the presence of titanite ($CaTiSiO_5$). Concurrently, the presence of Mn and Cl is suggestive of alteration processes and impurities affecting the calcite and pyroxene grains. The modal composition of JC is estimated to consist of 80% calcite, 17% pyroxene, 01% biotite, 01% apatite and < 01% opaque minerals.

Sillai Pattai (SP) carbonatites unveiled variations in the composition of rocks, primarily in terms of Ca, P, Fe, and Ti (Fig. 3b). Petrographic examination showed that SP carbonatites are characterized by mineral assemblage of calcite, apatite, amphibole, biotite, and opaque minerals (Fig. 4c-d). The modal abundance of SP carbonatites is exhibited by approximately 80% calcite, 11% apatite, 03% amphibole, 03% biotite and 02% opaque minerals. Preferred orientation of apatite, biotite, amphibole and opaque minerals and shearing in SP samples suggest these rocks underwent metamorphism or deformation that is evidenced also by distinctive arrangements of minerals and shearing at petrographic scale. Biotite shows alteration as evidenced by its transformation into vermiculite at places.

Loe Shilman (LS) carbonatites contain the dominant elements as Ca, P, Ti, and K, with rare Cl (Fig. 3c). In terms of petrography, the LS carbonatites primarily consist calcite, biotite, K-feldspar, amphibole and opaque minerals (including ilmenite, pyrochlore, and pyrite) accompanied by accessory minerals of apatite, titanite and zircon (Fig.

4e-f). According to the modal composition, LS carbonatites are composed of 95% calcite, 3% K-feldspar and 2% apatite. There is another variety of carbonatite with a different composition, featuring around 75% calcite, 10% opaque minerals, 10% biotite, and 5% amphibole. The apatite grains contain various minerals inclusions of zircon, rutile, and monazite.

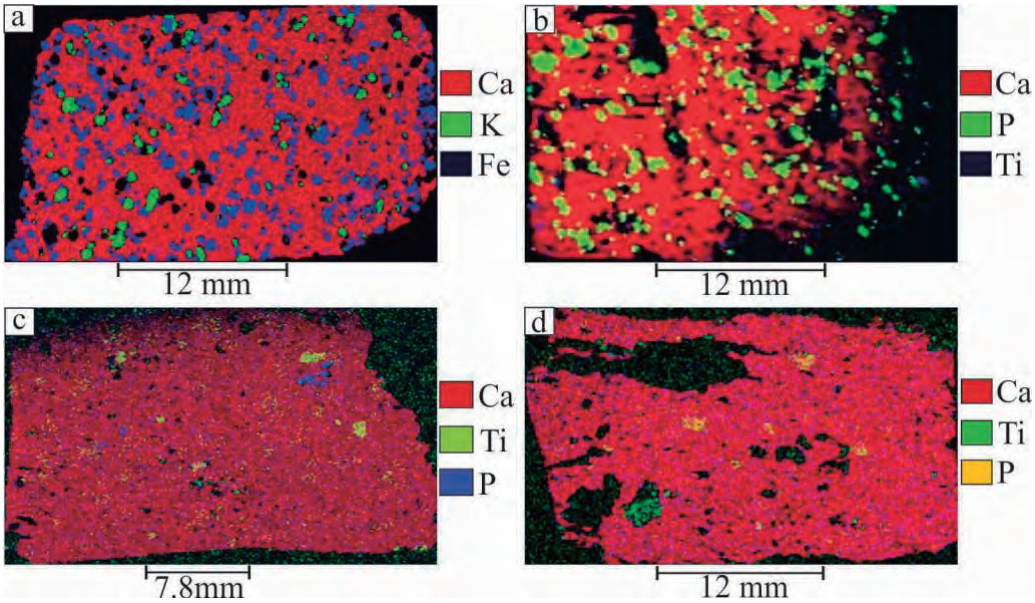

Fig. 3. Images of selected thin sections showing the elemental mapping obtained from the XGT analysis, a) Jambil carbonatites, b) Sillai Pattai carbonatites, c) Loe Shilman carbonatites, d) Warsak (Shina Gondai) carbonatites. Note a preferred orientation displayed by apatite grains in SP carbonatite sample, indicating their deformation due to metamorphic event.

Warsak (Shina Gondai: SG) carbonatites are highlighted by Ca, Fe, K, P and Ti as the dominant elements (Fig. 3d). In terms of petrology, the mineralogical variations observed include calcite, biotite, pyroxene, and opaque minerals (Fig. 4g-h). Additionally, less common minerals identified in this context are zircon and k-feldspar. According to the modal composition, SG carbonatites are primarily composed of 95% calcite, 2% biotite, 2% opaque minerals, and 1% pyroxene.

The HH-XRF analysis conducted on four carbonatite bodies showed elemental abundances of SiO_2, TiO_2, FeO, MgO, MnO, CaO, K_2O, Cr_2O_3, and P_2O_5 as shown in Table 1. In addition, minor and trace elements such as Cl, Ni, Cu, Zn, Rb, Sr, Y, Zr, Nb, Sn, Te, Ba, La, Ce, Pb, Th, U were also analyzed (Table. 2).

In the case of JC, the average CaO content exhibited a range of 38.4% to 44.3%, with an overall average of 38.9%. The SP carbonatite displayed a CaO range of 28.9% to 39.1%, with an average value of 34.9%. In the LS carbonatite, CaO levels ranged from 35.2% to 40.1%, with an average content of 37.7%. The SG carbonatite samples indicated CaO content ranging from 34.3% to 43.4%, with an average of 38.9%. The FeO content in JC varies from 0.7% to 1.3%, with an average of 01%. For SP, it falls within the range of 4.4% to 5.5%, with an average of 4.9%. LS exhibits a range of 1.5% to 5.9%, with an average content of 3.7%, while SG shows a range of 1.4% to 8.1%, with an average FeO content of 4.7%. The mean MnO content for JC stands at 0.1%, whereas for SP, it is 0.2%, and for both LS and SG, it reaches 0.3%. As for the average MgO content, JC contains 0%, SP has 2.2%, LS contains 1.3%, and SG holds 0.7%. The Al_2O_3 content is 0% in JC, 0.2% in SP, 0.3% in LS, and 1.4% in SG carbonatite (Table. 2). The LOI content for JC, SP, LS and SG is 52.35%, 46.2%, 48.4% and 50.6%, respectively.

The ternary diagram depicting CaO, MgO, and FeO reveals that all the studied carbonatite samples belong to the calcio carbonatite type, as they consistently plot at the apex within the CaO field (Fig. 5).

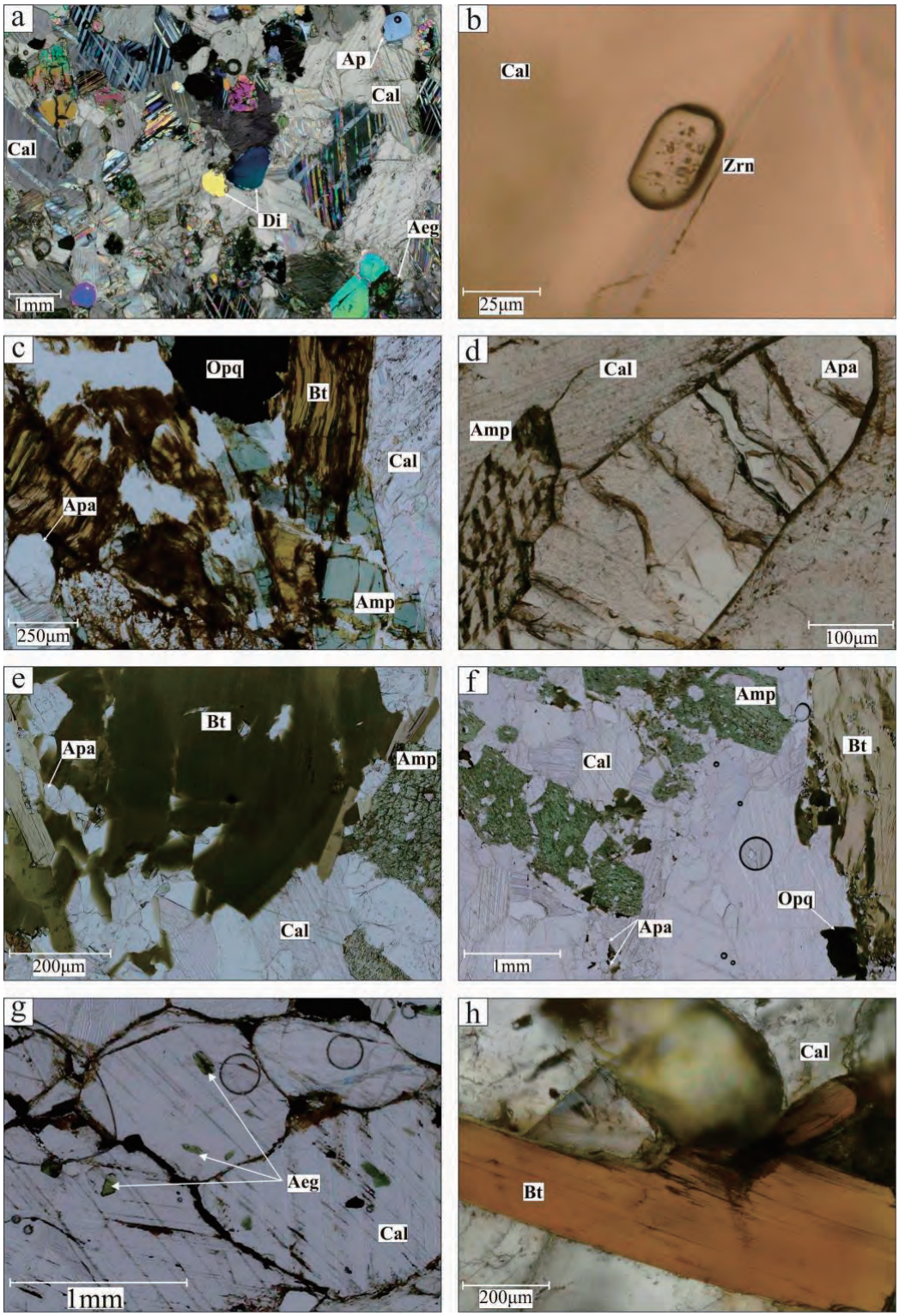

Fig. 4. Photomicrographs (taken under plane polarized nicols using the Keyence VHX-8000 digital microscope) of PPAIP carbonatites displaying petrographic details. a-b) Jambil carbonatites showing calcite, apatite, aegirine and accessory zircon, c-d) Sillai Pattai carbonatites showing calcite, apatite, biotite, amphibole and opaque minerals, e-f) Loe Shilman carbonatites with calcite, biotite and amphibole, g-h) Warsak carbonatites showing calcite with biotite and accessory aegirine.

4. Discussion

Petrological analyses of carbonatite samples from PPAIP reveal a change in mineral composition. All the studied carbonatites share a common calcio type, with calcite as the dominant phase. However, what sets them apart are the associated minerals that vary significantly among the samples. For instance, samples from JC are characterized by a dominance of pyroxene (mainly aegirine and diopside), while SP carbonatites exhibit an assemblage featuring apatite, biotite, amphibole, and opaque minerals. The LS carbonatites represent presence of biotite, amphibole, and opaque

Table 2. HH XRF analysis of carbonatites from PPAIP (major oxides in wt%, trace elements in ppm).

	Warsak		**Jambil**		**Loe Shilman**		**Sillai Pattai**			
	SG-10	SG-01	JC-03N	JC-03	LS-03	LS-01	SP-01A	SP-05	SP-M	SP-01
SiO_2	1.97	2.66	3.61	2.66	6.27	0.94	3.98	7.48	7.31	3.26
TiO_2	0.00	0.03	0.01	0.02	0.60	0.00	0.12	0.40	0.27	0.07
Al_2O_3	1.26	1.52	1.77	1.40	2.27	0.99	1.53	2.54	2.19	1.47
FeO	8.05	1.42	0.74	1.28	5.93	1.52	4.45	4.81	5.28	4.90
MgO	0.51	0.97	0.00	0.00	1.63	0.88	2.02	1.82	2.30	3.27
MnO	0.20	0.31	0.04	0.09	0.15	0.46	0.25	0.21	0.22	0.21
CaO	34.31	43.42	44.32	38.35	35.22	40.13	39.13	32.64	32.46	38.48
K_2O	0.14	0.35	0.24	0.06	1.12	0.13	0.07	0.86	0.79	0.06
Cr_2O_3	0.00	0.01	0.01	0.01	0.00	0.00	0.00	0.00	0.00	0.00
P_2O_5	0.34	0.60	0.45	0.38	3.21	1.91	3.66	2.10	2.43	3.83
Cl	0	6562	3832	1151	2810	3596	1999	1483	1338	2115
Ni	0.00	25.17	0.00	0.00	45.50	57.33	0.00	27.50	13.22	20.33
Cu	186.33	19.50	10.33	17.83	11.33	17.17	11.67	18.17	7.11	5.67
Zn	8.83	23.83	40.83	46.67	80.50	6.67	63.50	70.33	76.78	60.00
Rb	3.50	36.67	27.33	0.00	36.83	13.67	0.00	29.50	28.67	0.00
Sr	1145.33	3186.17	470.83	570.33	6670.83	9025.67	1184.67	5973.50	4740.11	4169.33
Y	42.17	83.33	12.00	11.67	60.67	83.50	79.33	89.83	82.11	80.33
Zr	0.00	0.00	30.50	0.00	191.67	0.00	304.83	0.00	179.78	70.00
Nb	0.00	0.00	0.00	0.00	0.00	66.83	0.00	12.17	133.67	0.00
Sn	77.17	67.50	58.83	81.33	104.17	86.50	78.83	74.83	73.56	93.33
Te	3.00	4.67	4.67	4.33	5.33	5.50	5.33	4.50	4.56	5.00
Ba	159.17	243.00	78.67	780.50	494.83	281.17	614.50	644.83	663.67	612.67
La	0.00	0.00	0.00	0.00	820.00	633.00	619.17	708.00	688.67	556.33
Ce	276.17	539.33	186.17	92.50	2285.00	2465.17	1449.00	1894.17	1784.78	1731.00
Pb	90.17	54.67	30.67	18.83	54.67	96.33	26.67	55.00	45.56	49.67
Th	0.00	7.00	0.00	0.00	43.33	36.17	7.67	26.00	21.44	21.67
U	0.00	0.00	0.00	0.00	0.00	68.00	0.00	0.00	20.78	0.00

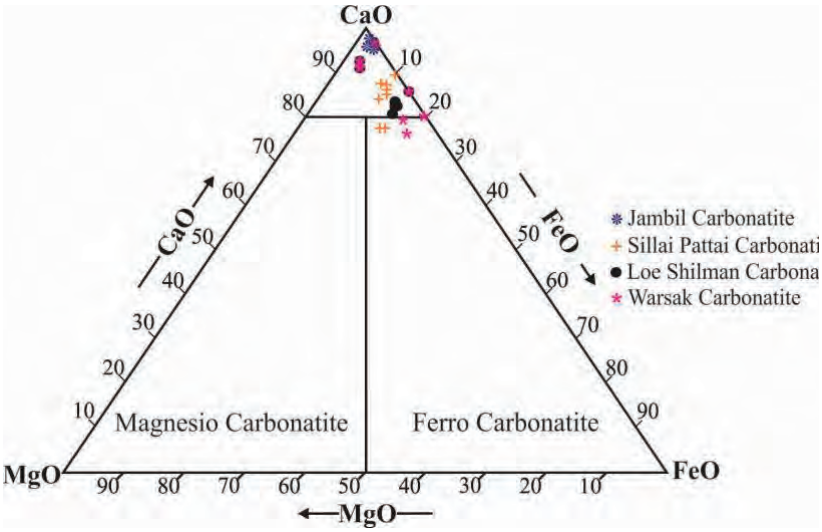

Fig 5. Analyzed samples plotted on a carbonatite ternary classification diagram after Wooley and Kemp [3].

minerals. The SG carbonatites display lower proportions of biotite and aegirine with minor amounts of opaque minerals. These variations suggest distinct geological processes, including fractional crystallization and assimilation, impacting each carbonatites mineral makeup. The different tectonic environments in which they were generated highlight diverse modes of crystallization and varying environmental conditions, offering valuable insights into their geological history and significance.

The JC carbonatites are intruded into Precambrian to Cambrian pelitic schist's and granitic gneisses [30,34,35]. The reported geochronological data from JC of ca. 438 ± 3 Ma and 15.7 ± 0.4 Ma [30,34] suggest significant temporal gap between the formation of the host rocks and the emplacement of the carbonatites. Geochemical results from JC reveal their parent magma had elevated concentrations of Ca^{+2}, K^{+2}, and Fe^{+2} cations. This composition led to the precipitation of the existing minerals in the JC. The presence of incompatible and trace elements resulted in the incorporation of various minerals, including zircon, rutile, and titanite.

The SP carbonatites were reported to have formed around 83 Ma (based on U–Pb titanite age), whereas other authors reported their magmatic age around 32 to 29 Ma (based on FT dating on apatite and zircon) [25,27,32]. These two different age values are challenging. Moreover, the compositional analysis of SP carbonatites reveal apatite, biotite, and amphibole as the dominant constituent phases. The presence of apatite in SP is intriguing and likely linked to late-stage geological events, either hydrothermal or thermal magmatic in nature, as discussed by Decrée et al. [36]. The apatite FT age of 29 Ma for the SP [32] and around 32 Ma [25] indicate thermal or metamorphic event or could be linked with their uplift and cooling . The preferred orientation of apatite within the SP carbonatites additionally implies their metamorphism that could have occurred during or after the India-Asia collision related tectonic event. It is important to understand the early crystallization-related event that generated the SP carbonatites and late-stage metamorphic events that deformed those rocks.

The LS carbonatites, exhibited by abundant Ca, P, Ti, and K, and U-Pb age of 90 Ma [28] suggest their more or less similar origin as that for the SP carbonatites. Similarly, the 30 Ma FT age from apatite [33] may indicate similar

scenario. The LS carbonatites intruded along the thrust sheet with Paleozoic sedimentary rock to the north and Precambrian slates and phyllite to the south [22]. The petrographic analysis of LS carbonatites revealing the presence of two dominant varieties: calcite-rich with no biotite and biotite-bearing types. This observation suggests that early-formed magma was the main body that formed biotite-absent carbonatites whereas the biotite could be a product of late-stage fluids that possibly infiltrated into the carbonatites. Further evidence supporting this hypothesis comes from age dating, with carbonatite samples showing age values of 90 Ma as the emplacement age and 30 Ma may indicate the potential influence of metamorphic and hydrothermal events. Overall, the petrographic and age data, coupled with the presence of specific minerals, underscore the multifaceted geological history and magmatic evolution of LS carbonatites, inviting further investigation and a deeper understanding of their formation processes.

The SG carbonatites are placed in the Warsak alkaline belt which consists of alkali granites, micro granites, albitites, and pyroxenites [4,23]. The discovery of SG carbonatites marks the first recorded occurrence of this rock type within the alkaline complex, and it had not been previously documented. Here the carbonatite is identified as a small vein-like structure, characterized by fresh, sugary-textured calcite, often accompanied by aegirine and biotite. Some sections of the carbonatites display oxidation, resulting in a brownish coloration. The predominance of calcite in the SG carbonatites suggests its origin from primary carbonatitic melt. Further investigation is needed to explore their tectonic, geodynamic, and mineralogical evolution.

5. Conclusions

This study of carbonatite occurences within the PPAIP has discussed mineralogical, textural, and compositional variations among the four carbonatite localities. The predominance of calcite in all four localities signifies their classification as calcio carbonatites, while associated minerals and elemental compositions exhibit significant diversity. The reported age data indicate varying geological histories for these carbonatites, with implications for their formation processes and late-stage tectonic events that modified them. The presence of minerals such as apatite, biotite, amphibole, and opaque minerals in studied carbonatites underscores the complex geological evolution they have undergone. Geochemical analyses highlight variations in major oxides and trace elements, shedding light on the petrogenesis of these carbonatites. Ternary diagrams affirm their classification as calcio carbonatites. This study contributes a petrological and geochemical perspective regarding the geological evolution of carbonatite bodies in the PPAIP. The ambiguity in geochronological data, the lack of clear tectonic settings that resulted these carbonatites and later deformed are the main questions that still remain and need further investigation.

Acknowledgements

The first author is grateful to MEXT Japan for the scholarship. We thank the staff of the Instrumental Analytical Center of the Kagoshima University for their assistance in analysis. RMu also appreciates the financial assistance provided to him by the Geological Survey of Pakistan for the fieldwork. Funds for the analysis were partly supported by the JSPS research grant (Kakenhi # 20K004135 to HUR).

6. References

[1] Woolley, A.; Church, A. Lithos 85 (2005) 1-14.
[2] Gibson, S. Le Maitre. Geological Magazine (2003) 140 357-367.

[3] Wooleby, A.; Kempe, D. Unwin Hyman (1989) 1-14.
[4] Le Bas, M. Geological Society London 30 (1987) 53-83.
[5] Yaxley, G.M.; Anenburg, M.; Tappe, S.; Decree, S.; Guzmics, T. Annual Review of Earth and Planetary Sciences 50 (2022) 261-293.
[6] Goodenough, K.M.; Deady, E.A.; Beard, C.D.; Broom-Fendley, S.; Elliott, H.A.; van den Berg, F.; Öztürk, H. Journal of Earth Science 32 (2021) 1332-1358.
[7] Woolley, A.R.; Kjarsgaard, B.A. The Canadian Mineralogist 46 (2008) 741-752.
[8] Vladykin, N.V.; Pirajno, F. Lithos 105982 (2021) 386-387.
[9] Chandra, J.; Paul, D.; Stracke, A.; Chabaux, F.; Granet, M. Journal of Petrology 60 (2019) 1119-1134.
[10] Løvik, A.N.; Hagelüken, C.; Wäger, P. Sustainable Materials and Technologies 15 (2018) 9-18.
[11] Woolley, A.R. Geological Survey of Canada Open File (2008) 1-30.
[12] Kumar, A.; Charan, S.N.; Gopalan, K.; Macdougall, J. Geochimica et Cosmochimica Acta 62 (1998) 515-523.
[13] Deans, T.; Powell, J. Nature 218 (1968) 750-752.
[14] Schleicher, H.; Todt, W.; Viladkar, S.G.; Schmidt, F. Chemical Geology 140 (1997) 261-273.
[15] Sorokhtina, N.; Belyatsky, B.; Zaitsev, V.; Viladkar, S.; Kononkova, N.; Ghatak, A. Geochemistry International 60 (2022) 1237-1261.
[16] Sarkar, A.; Datta, A.; Poddar, B.; Bhattacharyya, B.; Kollapuri, V.; Sanwal, R. Journal of Southeast Asian Earth Sciences 13 (1996) 77-81.
[17] Fosu, B.R.; Ghosh, P.; Chew, D.M.; Viladkar, S.G. Geological Journal 54 (2019) 3438-3454.
[18] Weerakoon, M.; Miyazaki, T.; Shuto, K.; Kagami, H. Gondwana Research 4 (2001) 409-420.
[19] Manthilake, M.; Sawada, Y.; Sakai, S. Journal of Asian Earth Sciences 32 (2008) 66-75.
[20] Tucker, R.D.; Belkin, H.E.; Schulz, K.J.; Peters, S.G.; Buttleman, K. US Geological Survey report (2011).
[21] Randive, K.; Meshram, T. Open Geosciences 12 (2020) 85-116.
[22] Le Bas, M.; Mian, I.; Rex, D. Geologische Rundschau 76 (1987) 317-323.
[23] Kempe, D.R.C.; Jan, M.Q. University of Peshawar (1980).
[24] Jan, M.Q.; Karim, A. Journal Of Himalayan Earth Sciences 23 (1990) 43 -49.
[25] Butt, K.; Arif, A.Z.; Ahmed, J.; Ahmed, A.; Qadir, A. Journal of Himalayan Earth Sciences 22 (1989) 197-215
[26] Kempe, D. Geological Magazine 110 (1973) 385-404.
[27] Zhu, Y.-X.; Wang, L.-X.; Khattak, N.U.; Ma, C.-Q.; Luo, G.-M.; Ulrich, T. Lithos 107087 (2023) 442-443.
[28] Khan, A.; Faisal, S.; Larson, K.P.; Robinson, D.M.; Ullah, Z.; Li, H.; Rehman, H.U. Lithos 106497 (2021) 404-405.
[29] Aslam, M.; Hussain, A.; Ashraf, M.; Afridi, A.G.K Geological Survey of Pakistan Map seies (2006).
[30] Khattak, N.; Qureshi, A.; Akram, M.; Ullah, K.; Azhar, M.; Khan, M.A. Journal of Asian Earth Sciences 25 (2005) 643-652.
[31] Qureshi, A.; Butt, K.; Khan, H. International Journal of Radiation Applications and Instrumentation 18 (1991) 315-319.
[32] Khattak, N.; Khan, M.A.; Ali, N.; Abbas, S.; Tahirkheli, T. Russian Geology and Geophysics 53 (2012) 736-744.
[33] Khattak, N.; Akram, M.; Khan, M.; Khan, H. Radiation Measurements 43 (2008) 313-318.
[34] Khan, A.; Faisal, S.; Larson, K.P.; Robinson, D.M.; Li, H.; Ullah, Z.; Button, M.; Nawab, J.; Farhan, M.; Ali, L. Journal of Earth Science 34 (2023) 70-85.
[35] Khan, R.N.; Iqbal, S.; Khan, S.; Aslam, M Geological Survey of Pakistan Map series (1995).
[36] Decrée, S.; Savolainen, M.; Mercadier, J.; Debaille, V.; Höhn, S.; Frimmel, H.; Baele, J.-M. G. Applied Geochemistry 123 (2020) 1-17.